Hindawi
Wireless Communications and Mobile Computing
Volume 2022, Article ID 5853561, 11 pages
https://doi.org/10.1155/2022/5853561

Research Article

Research and Application of Color of Qiuci Murals Based on Intelligent Digital Image Processing Technology

Qianqian Kong[1] **and Yong Qiao**[2]

[1]*College of Fine Arts, Xinjiang Normal University, Urumqi, Xinjiang 830054, China*
[2]*Beijing DiDi Infinity Technology and Development Company Ltd., Beijing 100085, China*

Correspondence should be addressed to Qianqian Kong; 107622018070019@xjnu.edu.cn

Received 8 March 2022; Revised 11 April 2022; Accepted 21 April 2022; Published 14 May 2022

Academic Editor: Mu En Wu

In order to improve the color research effect of Qiuci murals, this paper combines digital technology, applies intelligent digital image processing technology to the color research of Qiuci murals, and builds an intelligent system. Moreover, this paper analyzes the color mural pixel digitization of murals from the perspective of digitization and conducts research from a microscopic perspective. In addition, in this paper, the expansion operation is performed for particularly small cracks, and the extraction area of the crack is correspondingly increased, which reduces the bad influence on the subsequent repair due to incomplete crack extraction. Finally, this paper constructs an intelligent mural analysis system based on the improved algorithm. The experimental research results show that the color research system of Qiuci murals based on intelligent digital image processing technology proposed in this paper has good effects and can play an important role in the digital protection and digital restoration of art.

1. Introduction

The Qiuci Grottoes are an important part of ancient Chinese Buddhist grottoes. Guguizi Kingdom is located in the center of the northern Silk Road south of Tianshan, including today's Kuqa, Shaya, Xinhe, Baicheng, and Luntai. Ancient Qiuci is an important area for the growth, dissemination, and development of Buddhist art in Xinjiang, where Buddhism was once extremely popular. Documents record that "Qiuci has a city outline, its city is triple, and there are thousands of Buddhist pagodas and temples." Therefore, this area is widely distributed with grotto groups. The famous Qiuci Grottoes preserved so far include Kizil Grottoes and Wenbashi Grottoes in Baicheng County; Kumtula Grottoes, Senmusem Grottoes, Kizilgaha Grottoes, Bostan Togra Grottoes, and Aai Grottoes in Kuqa County; and Tuohulak Aiken Grottoes in Xinhe County. There is no exact information on the founding time of the Qiuci Grottoes, but they were generally excavated and constructed from the Eastern Han dynasty to the Tang and Song dynasties. There are still 166 caves with murals preserved in the Qiuci Grottoes, among which the murals in the Kizil Grottoes are the most well-preserved, about 10,000 square meters. The unique artistic value of the murals in the Qiuci Grottoes lies in that they not only have the distinctive cultural characteristics of the Western Regions but also integrate the elements of the Han culture in the Central Plains and include elements of the Indian and Persian cultures. Moreover, the murals are diverse in content and skilled in drawing and have outstanding and unique artistic effects. The murals of the Qiuci Grottoes are an important part of the art and culture of Chinese Buddhist grottoes and also an indispensable content for the study of the history of ancient Chinese art and decorative art.

The colors of Qiuci murals are elegant and rich, with strong contrast and dazzling brilliance. The color of the mural does not come from the real color in reality, but from the abstract cognitive concept, and is limited by the existing pigment varieties at the time. There are often only a few colors in the mural works, and the configuration is relatively fixed, but the ancients created the infinite in the limited,

using the color combination of cool, warm, and fresh gray and the distribution of large and small areas to organize a rich color relationship. The color of Qiuci murals makes full use of the function of color symbolism to express the artistic conception of Buddhism. The formation of a nation's color concept is affected by the regional environment, history, folk customs, and traditional cultural concepts. These factors influence their observation and understanding of color, thus affecting the aesthetics and application of color. The main colors of Qiuci murals are blue, green, red, black, and white, and various changes have evolved on these five keynotes. The Qiuci area has a hot climate and a large temperature difference between day and night; it is rich in geological features, including deserts, Gobi, mountains, plains, and oases; it is located at the transportation hub between China and the west on the Silk Road and is one of the four major cities of ancient India, Greece-Roman, Persia, and Han and Tang dynasties. The intersection of civilizations is impacted and influenced by multiple cultures. These factors contribute to the exotic high purity and strong contrast of the colors of the Qiuci frescoes. In Buddhist culture, blue symbolizes the light that drives away all darkness. The lapis lazuli, which was introduced from Afghanistan through the Silk Road, has a strong and pure color, is gorgeous and noble, and can be divided into dark blue, purple blue, sky blue, green blue, etc., which well interprets the theme of Buddhist compassion and peace and becomes a natural blue pigment. The main raw material of Qiuci is much favored by Qiuci artists. Green represents the vegetation and water that the Qiuci people advocated. Islamic art came from the Silk Road, and a large number of turquoise materials were also introduced. Red symbolizes good luck and blessing, and the Grand Canyon in Aksu region provides a lot of rich red pigments for murals. White represents purity and holiness. Black is a symbol of holiness, luck, and power. The blue-green contrast, red-blue contrast, red-green contrast, and other color contrast relationships in the murals make the picture clear, gorgeous, and unified, and use the color language to directly convey the spiritual connotation.

This paper combines digital technology to apply intelligent digital image processing technology to the color research of Qiuci murals, constructs an intelligent system, and provides a theoretical reference for the color research of Qiuci murals and its extended application.

2. Related Work

Murals are the combination of "wall" and "painting." As the name suggests, it is a painting made on the wall through painting and craftsmanship. In general, murals originally refer to flat static paintings, which have the functions of narrative, publicity, education, and decoration. However, with the development of the times, people's dependence on modern new media art has gradually increased, and the expression form of traditional mural art is obviously not enough to attract the sensory needs of modern people [1]. Therefore, traditional mural art is facing a situation that needs to be "updated and upgraded." Openness is the main feature of digital mural art, which means that in the creation of murals, its own creative process, cultural concepts, aesthetic activities, and values are open [2]. The second is diversity, which is mainly reflected in the diversity of production methods, media methods, and artistic styles [3]. Among them, the medium of murals is no longer just a two-dimensional plane that can be painted on the wall but can be presented on a certain surface through three-dimensional and projection technology. In terms of artistic style, different historical periods, regional cultures, materials and craftsmanship, and diverse space requirements make modern mural art present diverse styles [4]. Compared with traditional murals, the concept of murals today may be gradually transformed from static two-dimensional plane paintings to three-dimensional, dynamic, and interactive forms of expression [5]. After being combined with modern digital technology, it can not only break through people's visual senses but also strengthen the promotion of traditional culture and make it easier for us to update and maintain it [6]. With the development of society and people's higher demand for spiritual life, more rich and interesting mural art forms will be born [7].

The mural art under the digital background is a relationship of inheritance and development to the traditional form of murals, and the two are inseparable [8]. The mural art under the digital background also involves many aspects of traditional aesthetic thought [9]. In traditional art, murals pay special attention to the expression of art forms, and the beauty of nature is not simply a sensory experience for the author, but more importantly, the existence of order [10]. On the basis of absorbing the essence of traditional aesthetics, modern mural art brings people a brand-new visual beauty with its unique visual form [11]. With the rapid advancement of science and technology, new media art is quietly changing people's thinking and way of life. Artists integrate the spirituality and beauty of art into modern murals to create modern murals with the characteristics of the times, which promotes the harmonious and unified development of technology and art [12]. In the creation and implementation of modern mural art, the relationship between time and space can be handled very freely. This form of artistic expression is created, communicated, and appreciated through imagination, with hazy images and specific external objects and scenery. Second, there is the difference in performance methods [13]. In literature [14], "Science can make people fall in love with what suits their temperament according to their own preferences, especially to study what is most consistent with his spirit." Humans have changed from simply imitating traditional media to using computers and in computers create or automatically generate to achieve the desired artistic effect. The popularity of computers and their simple operability makes the use of computers no longer unfamiliar to artists and gradually turns computers into the most basic tools and media in artistic creation. Art is creation, a community of imagination and emotion. Although it is necessary for authors and viewers to be active, creation requires the support of media to be realized. Without this logic, artistic creation and appreciation cannot be guaranteed [15]. In the process of art creation, it is not difficult to find that new technologies have contributed to the change of media, and the relationship between media

and artistic expression has become the most common problem in art research [16]. Although digital new media art and traditional art are strongly related, it is obvious that they are based on their own creative interface and existing space. If traditional mural art is the embodiment of nature, it is an artistic creation that combines traditional culture and is based on manual skills and presented in the form of physical objects, and then, modern murals use advanced digital technology and software graphics processing tools and other advanced tools. The technique of fresco creation is essentially different from the traditional fresco technique only in the difference of the medium and tools of expression [17].

Today, the rapid development of digital media has brought new prospects and development directions to traditional mural art. Among the ancient Chinese religious sites that have been preserved so far, the temple murals in Shanxi are second to none. However, nowadays, the prospect of traditional temple murals in Shanxi is very worrying. Due to the different economic conditions, technical strength, and importance of cultural relics in different places, the local cultural relic protection departments are overwhelmed and neglected in management and development [18]. The top priority is not only to protect most of the ancient murals but also to better carry forward and inherit. Nowadays, murals are no longer a simple cultural carrier and will gradually become a new type of communication medium with the changes of the times [19].

3. Intelligent Digital Image Processing Technology

From the perspective of digitization of the color mural pixels of the murals, the research is carried out from a microscopic perspective. In fresco color, we consider a three-energy Λ -type fresco pixel with two simplicial ground states $|g_+\rangle_1$ and $|g_-\rangle_1$ and excited state $|e\rangle_1$, and a three-energy V-type fresco pixel with two simplicial excited states $|e_+\rangle_2$ and $|e_-\rangle_2$ and ground state $|g\rangle_2$. Both of these mural pixels are captured in a dual-mode cavity, as shown in Figure 1.

Under the dipole approximation and the rotating wave approximation, the Hamiltonian of the system is ($\hbar = 1$).

$$H_2 = H_0 + H_1,$$
$$H_0 = \sum_{j=\pm}\left(\omega_1\sigma_{1,j}^z + \omega_2\sigma_{2,j}^z + \omega_j a_j^\dagger a_j\right). \quad (1)$$

$$H_1 = \sum_{j=\pm}\left(g_1 a_j\sigma_{1,j}^+ + g_2 a_j\sigma_{2,j}^+\right) + H.c. \quad (2)$$

where $H.c.$ represents the Hermitian conjugate, H_0 represents the free energy of the cavity mode and the mural pixel, and H_1 describes the interaction between the mural pixel and the cavity mode. $a_j^\dagger$ and a_j are the production and annihilation operators for photons of frequency ω_j, respectively. Polarization "+" and "-" represent left-handed and right-handed polarizations, respectively. Among them, the fresco pixel operators are defined as $\sigma_{1,j}^z = (|e\rangle_{11}|e| - |g_j\rangle_{11}\langle g_j|)/2$, $\sigma_{2,j}^z = (|e_j\rangle_{22}\langle e_j| - |g\rangle_{22}\langle g|)/2$, $\sigma_{1,j}^+ = |e\rangle_{11}\langle g_j|$ and $\sigma_{2,j}^+ = |e_j\rangle_{22}\langle g|$, where ω_1 and ω_2 are the resonant frequencies of transitions $|e\rangle_1 \longrightarrow |g_j\rangle_1$ and $|e_j\rangle_2 \longrightarrow |g\rangle_2$, respectively, and g_1 and g_2 are variable coupling constants. Here, we assume that the left-handed and right-handed polarized cavity modes have the same frequency ω, and the mural pixel and the cavity mode are resonantly interacting, that is, $\omega_\pm = \omega_1 = \omega_2 = \omega$.

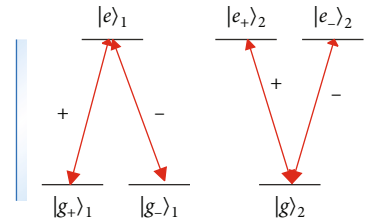

Figure 1: Schematic illustration of a three-level Λ-type mural pixel and a three-level V-type mural pixel trapped in a dual-mode cavity.

In the interaction picture, the Hamiltonian of the system is [20]

$$H_3 = \sum_{j=\pm}\left(g_1 a_j\sigma_{1,j}^+ + g_2 a_j\sigma_{2,j}^+\right) + H.c. \quad (3)$$

First, we describe the generation process of the entangled state $1/\sqrt{2}(|g_+\rangle_1|e_+\rangle_2 + |g_-\rangle_1|e_-\rangle_2)$ between two mural pixels in the above system. Initially, the cavity field is in a vacuum state, the mural pixel 1 is in the excited state $|e\rangle_1$, and the mural pixel 2 is in the ground state $|g\rangle_2$. Since the spontaneous emission mural pixel point 1 radiates a photon, this photon may be a left-handed polarized photon "+" or a right-handed polarized photon "-". Moreover, after the photons are radiated, the state of the mural pixel becomes $|g_+\rangle_1$ or $|g_-\rangle_1$ correspondingly. The radiated photons may be absorbed by the mural pixel 2. After absorbing this photon, the state of the mural pixel 2 may be $|e_+\rangle_2$ or $|e_-\rangle_2$. It is through this process that the corrected state $1/\sqrt{2}(|g_+\rangle_1|e_+\rangle_2 + |g_-\rangle_1|e_-\rangle_2)$ of the two mural pixels is generated.

The state of the whole system is related to a subspace with only one excitation number, and the basis vector of this subspace is

$$|1\rangle = |e\rangle_1|g\rangle_2|0\rangle, |2\rangle = |g_+\rangle_1|g\rangle_2|1_+\rangle, |3\rangle = |g_-\rangle_1|g\rangle_2|1_-\rangle,$$
$$|4\rangle = |g_+\rangle_1|e_+\rangle_2|0\rangle, |5\rangle = |g_-\rangle_1|e_-\rangle_2|0\rangle, \quad (4)$$

where $|0\rangle$ represents the vacuum state of the cavity field and $|1_+\rangle$ and $|1_-\rangle$ represent the states of photons with a left-handed polarization in the cavity and a right-handed polarization in the cavity, respectively. The state vector of the

system can be expanded by the basis vector above as

$$|\Psi(t)\rangle = \sum_{k=1}^{5} C_k(t)|k\rangle, \tag{5}$$

where $C_k(t)(k = 1 - 5)$ is the probability amplitude of state $|k\rangle$. Using the basis vectors in equation (4), the Hamiltonian of the system can be written in the form of a matrix. The state corresponding to the zero eigenvalue of the Hamiltonian of the system can be obtained by calculation. Generally, we call such a state a dark state, and its specific form is

$$|D_1(t)\rangle = \frac{1}{\sqrt{2}} \sin\theta(|g_+\rangle_1|e_+\rangle_2 + |g_-\rangle_1|e_-\rangle_2)|0\rangle - \cos\theta|e\rangle_1|g\rangle_2|0\rangle. \tag{6}$$

Among them, there are

$$\sin\theta = \frac{\sqrt{2}g_1}{\sqrt{2g_1^2 + g_2^2}}, \qquad \cos\theta = \frac{g_2}{\sqrt{2g_1^2 + g_2^2}}. \tag{7}$$

At the initial moment, we choose $g_2 \gg g_1$; then, there is $\cos\theta = 1$. Then, the state of the whole system is $|D_1(0)\rangle = |e\rangle_1|g\rangle_2|0\rangle$ at this time.

$$\lim_{t\longrightarrow-\infty} \frac{g_1(t)}{g_2(t)} = 0, \qquad \lim_{t\longrightarrow+\infty} \frac{g_2(t)}{g_1(t)} = 0. \tag{8}$$

If we define the pulse sequence above, we can adiabatically transfer the entire system from the initial state $|D_1(0)\rangle$ to the following state:

$$|D_1(T_1)\rangle = \frac{1}{\sqrt{2}}(|g_+\rangle_1|e_+\rangle_2 + |g_-\rangle_1|e_-\rangle_2)|0\rangle, \tag{9}$$

where T_1 is the time required to complete this adiabatic evolution, and we will show how to estimate this time T_1 later. After the above operations, the two mural pixels 1 and 2 are prepared in a maximum entangled state of the two mural pixels, and the cavity field remains in its vacuum state $|0\rangle$. In order to preserve the entangled state we obtained, we can transfer the mural pixel point to its metastable state in time. To accomplish this operation, we apply a π-polarized light to transitions $|e_\pm\rangle_2$ and $\langle g_{\pm_2}$ to transfer the entangled state of the two mural pixels obtained above to a more stable entangled state: $\psi_{12} = 1/\sqrt{2}(|g_+\rangle_1|g_+\rangle_2 + |g_-\rangle_1|g_-\rangle_2)$. After the interaction is over, we can do a joint Bell state measurement to demonstrate the entanglement between mural pixels 1 and 2.

Next, we introduce how to get the pulse sequence we need by choosing the number of properly. As shown in

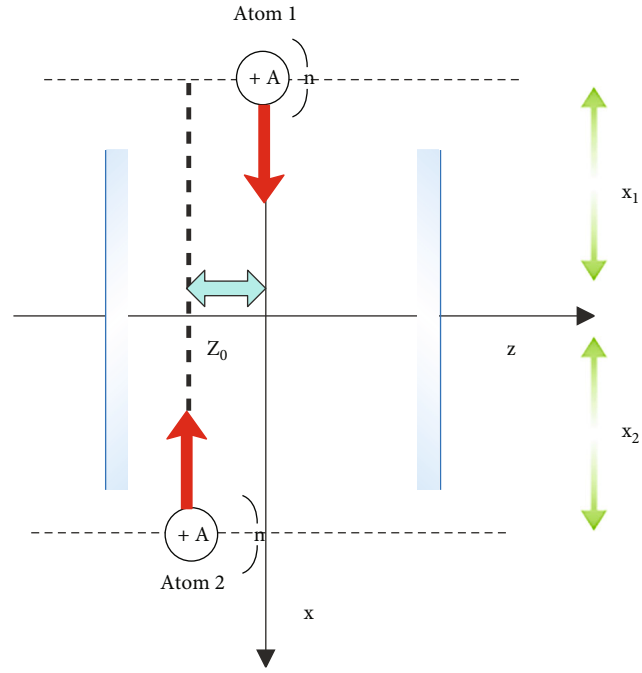

Figure 2: Schematic diagram of the motion trajectory of the pixel points in the intracavity mural.

Figure 2, the cavity field is initially in a vacuum state, the Λ-shaped mural pixel point 1 enters the cavity from the $y = 0$ plane along the $z = 0$ line at a speed v, and the V-shaped mural pixel 2 enters the cavity field along the $z = z_0$ line from the $y = 0$ plane at a speed v in the opposite direction of the motion of the mural pixel 1. The time-dependent Rabi frequency is

$$g_1(t) = g_{10}\exp\left(-(vt)^2/W_c^2\right), \qquad g_2(t) = g_{20}\exp\left(-v^2(t+\tau)^2/W_c^2\right)\cos\left(\frac{2\pi z_0}{\lambda}\right). \tag{10}$$

Here, we define the moment when the mural pixel 1 moves to the center of the cavity $x = 0$ as the origin of time $t = 0$. The initial x-coordinates of the two mural pixels are x_1 and x_2, respectively. g_{10} and g_{20} are the maximum values of $g_1(t)$ and $g_2(t)$, respectively, and the parameter W_c is the waist of the cavity.

Figure 3(a) scii frequency of the cavity mode with time, and Figure 3(b) shows the variation curve of the population with time. The pulse parameters are chosen as $z_0 = 0$, $g_{10} = g_{20} = 25\Gamma$, $\tau = 1.25\Gamma^{-1}$, and $W_c = 10\Gamma^{-1}$, wavelength is $\lambda = 852.36$ nm and $v = 20$ m/s, and the spontaneous emission decay rate of mural pixels is $\Gamma/2\pi = 5$ MHz. It can be clearly seen from the figure that all the populations are transferred from the initial state $|1\rangle = |e\rangle_1|g\rangle_2|0\rangle$ to the entangled state $|D_1(T_1)\rangle = 1/\sqrt{2}(|g_+\rangle_1|e_+\rangle_2 + |g_-\rangle_1|e_-\rangle_2)|0\rangle$ of the mural pixels. After applying the transfer pulse from the mural pixels to the metastable state, all the populations will be transferred to the stable maximum correction state of the two mural pixels $1/\sqrt{2}(|g_+\rangle_1|g_+\rangle_2 + |g_-\rangle_1|g_-\rangle_2)$. This shows

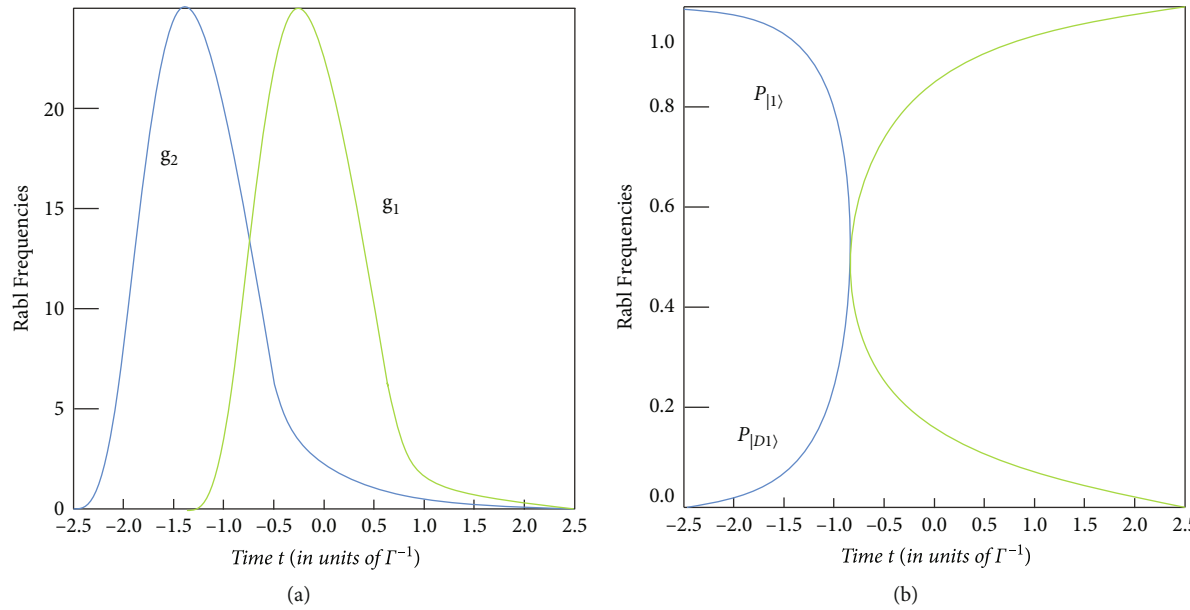

Figure 3: (a) Rabi frequency of cavity mode versus time. (b) Population evolution over time.

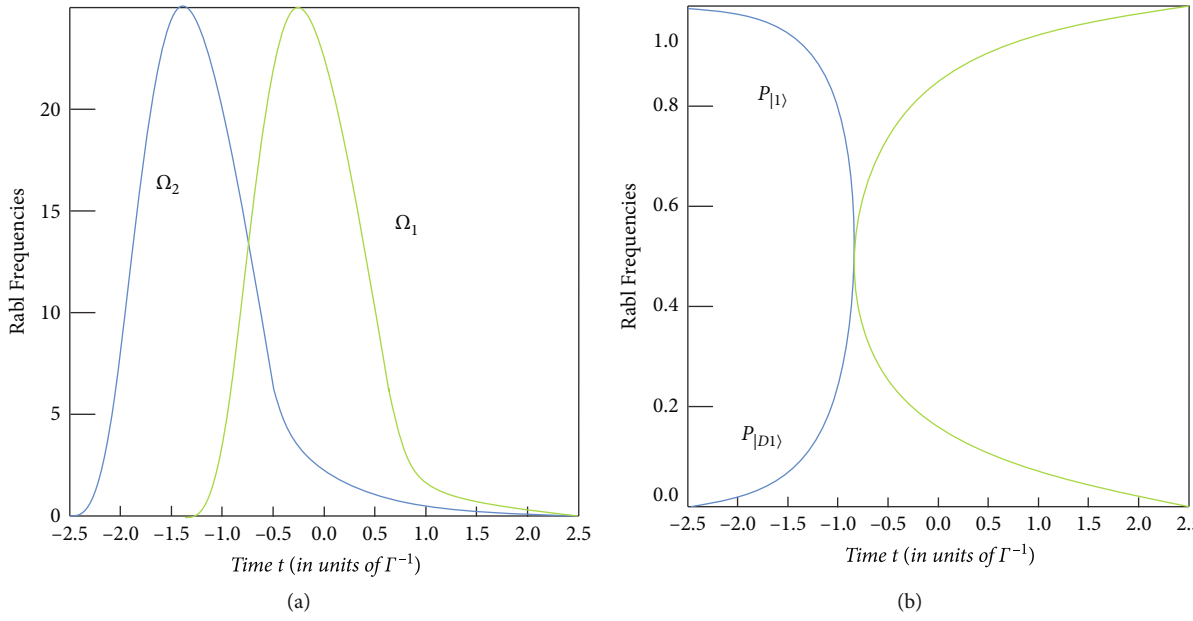

Figure 4: (a) The Rabi frequency of the cavity mode varies with time, where the selection of the pulse parameters is the same as that in Figure 3(a). (b) The evolution of the population with time when $N = 4$.

that we obtain the maximum rectification state of the two mural pixels from the initial state of the mural pixels by the adiabatic evolution method.

Next, we introduce how to generate the W state of N mural pixels. We assume that there are $N + 1$ mural pixels, one of which is a three-level Λ-type mural pixel, and the remaining N are three-level V-type mural pixels. The mural pixel system we describe here is the same as the previous mural pixel energy level in the two-mural pixel maximum entangled state scheme. We mark the Λ -shaped mural pixel as the $N + 1$-th mural pixel. Among them, the two degenerate ground states are $|g_+\rangle_{N+1}$ and $|g_-\rangle_{N+1}$, and their excited states are $|e\rangle_{N+1}$, while the two degenerate excited states of the NV-shaped mural pixels are $|e_+\rangle_j$ and $|e_-\rangle_j$, their ground states are $|g\rangle_j$, and $(j = 1, 2\cdots, N)$. The $N + 1$ mural pixels are also captured in a dual-mode cavity. We assume that the $(N + 1)$ mural pixels experience the same field and that two adjacent mural pixels are far enough apart that the dipole-dipole interaction between them is negligible.

In the above figure, the selection of pulse parameters is $z_0 = 0$, $g_{10} = g_{20} = 25\Gamma$, $\tau = 1.25\Gamma^{-1}$, and $W_c = 10\Gamma^{-1}$, wavelength is $\lambda = 852.36$ nm and $v = 20$ m/s, and the spontaneous emission decay rate of mural pixels is $\Gamma/2\pi = 5$ MHz.

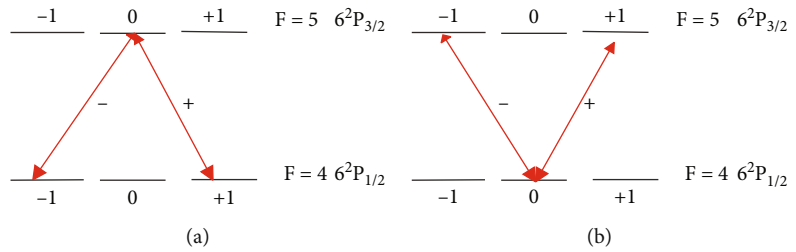

FIGURE 5: (a) Schematic diagram of the interaction between the Λ-shaped mural pixels and cavity modes in ^{133}Cs and (b) schematic diagram of the interaction between V-shaped mural pixels and cavity modes in ^{133}Cs.

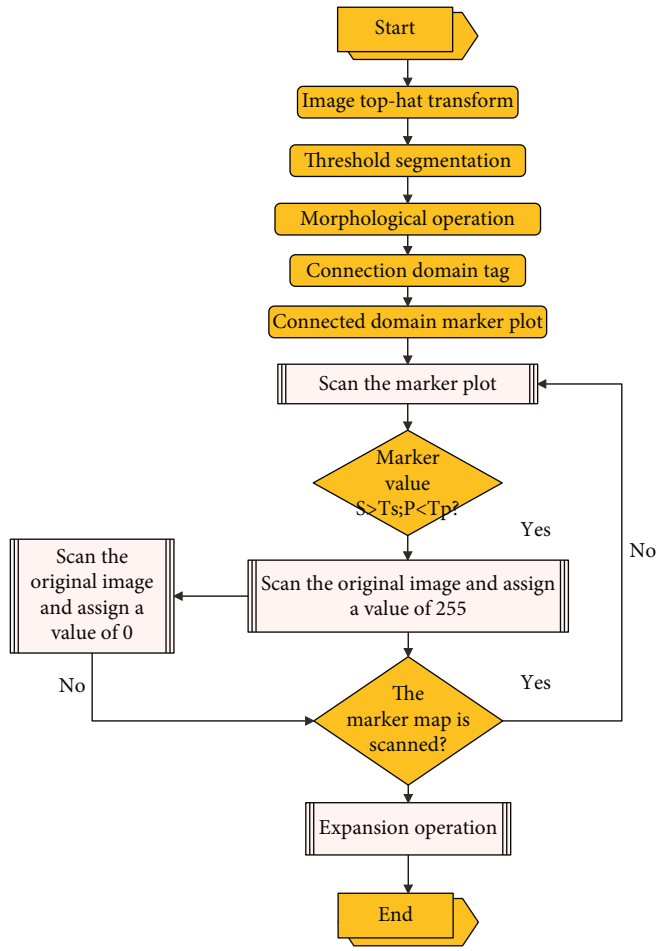

FIGURE 6: Extraction algorithm.

We assume that the frequencies of the two cavity modes are the same and that they both interact with the atomic resonance. In the interaction picture, under the dipole approximation and the rotational wave approximation, the Hamiltonian of the system of the mural pixel point and the cavity field is

$$H_4 = \sum_{j=\pm} \left(\Omega_1 a_j \sigma^+_{N+1,j} + \Omega_2 a_j \sum_{k=1}^{N} \sigma^+_{k,j} \right) + H.c. \tag{11}$$

Here, we assume that all NV-shaped mural pixels have the same coupling constant Ω_2, and the coupling constant of the $(N+1)$-th mural pixel is Ω_1. In order to understand this scheme more clearly, let us first introduce the formation process of entanglement. We assume that the initial state of the system is $|e\rangle_{N+1}|g\rangle_1|g\rangle_2 \cdots |g\rangle_N|0\rangle_0$, and the $(N+1)$-th mural pixel that is initially in the excited state will radiate a photon with a polarization mode of "+" or "-", and the state of the mural pixel after radiation change to $|g_+\rangle_{N+1}$ or $|g_-\rangle_{N+1}$. The radiated photon may be absorbed by the remaining NV-shaped mural pixels. Since the N mural pixels are exactly the same, their probability of absorbing the radiated photons is also exactly the same. This is also

the essential reason why the W state of N mural pixels can be generated in this system. Once the $j(j = 1, 2 \cdots N)$-th mural pixel absorbs the radiated photon, it will be excited to the $|e_+\rangle_j$ or $|e_-\rangle_j$•N mural pixel W state. This is how it is generated.

The state of the whole system belongs to a subspace with only one excitation number, and the basis vector of this subspace is

$$\begin{aligned} |1\rangle &= |e\rangle_{N+1}|g\rangle_1|g\rangle_2 \cdots |g\rangle_N|0\rangle, \\ |2\rangle &= |g_+\rangle_{N+1}|g\rangle_1|g\rangle_2 \cdots |g\rangle_N|1_+\rangle, \\ |3\rangle &= |g_-\rangle_{N+1}|g\rangle_1|g\rangle_2 \cdots |g\rangle_N|1_-\rangle, \\ |4\rangle &= |g_+\rangle_{N+1}|W_+\rangle_N|0\rangle, \\ |5\rangle &= |g_-\rangle_{N+1}|W_-\rangle_N|0\rangle. \end{aligned} \tag{12}$$

Among them, there are

$$|W_\pm\rangle_N = \frac{1}{\sqrt{N}}(|e_\pm\rangle_1|g\rangle_2 \cdots |g\rangle_N + |g\rangle_1|e_\pm\rangle_2 \cdots |g\rangle_N + \cdots + |g\rangle_1|g\rangle_2 \cdots |e_\pm\rangle_N), \tag{13}$$

where $|W_\pm\rangle_N$ is the entangled state of N mural pixels, that is, the W state of N mural pixels, which means that one of the N mural pixels is in $|e_\pm\rangle_j$, and the rest of the mural pixels are in the ground state. Using this basis vector, the state vector at any time t can be expanded as

$$|\Phi(t)\rangle = \sum_{k=1}^{5} C_k'(t)|k\rangle, \tag{14}$$

where $C_k'(t)(k = 1 - 5)$ is the expansion coefficient of the state $|k\rangle$. Using the above basis vectors, the Hamiltonian of the system can be written in the form of a matrix, and the calculation finds that the system has a state with zero eigenvalues, that is, a dark state. The dark state has the form

$$\begin{aligned} |D_2(t)\rangle = \frac{1}{\sqrt{2}} &\sin\phi(|g_+\rangle_{N+1}|W_+\rangle_N + |g_-\rangle_{N+1}|W_-\rangle_N)|0\rangle \\ &- \cos\phi|e\rangle_{N+1}|g\rangle_1|g\rangle_2 \cdots |g\rangle_N|0\rangle. \end{aligned} \tag{15}$$

Among them, there are

$$\begin{aligned} \sin\phi &= \frac{\sqrt{2}\Omega_1}{\sqrt{2\Omega_1^2 + N\Omega_2^2}}, \\ \cos\phi &= \frac{\sqrt{N}\Omega_2}{\sqrt{2\Omega_1^2 + N\Omega_2^2}}. \end{aligned} \tag{16}$$

At the initial moment, we choose $\Omega_2 \gg \Omega_1$ and then $\cos\phi = 1$. At this time, the system is in the dark state $|D_2(0)\rangle = |e\rangle_{N+1}|g\rangle_1|g\rangle_2 \cdots |g\rangle_N|0\rangle$. The following pulse train is selected.

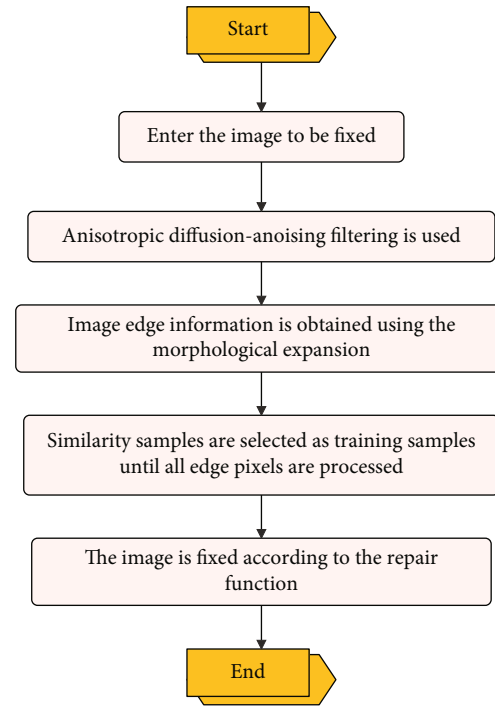

Figure 7: The color restoration process of Qiuci murals based on intelligent digital image processing technology.

$$\begin{aligned} \lim_{t\longrightarrow-\infty}\frac{\Omega_1(t)}{\Omega_2(t)} &= 0, \\ \lim_{t\longrightarrow+\infty}\frac{\Omega_2(t)}{\Omega_1(t)} &= 0. \end{aligned} \tag{17}$$

The initial state $|D_2(0)\rangle$ of the system evolves adiabatically to the following states:

$$|D_2(T_2)\rangle = \frac{1}{\sqrt{2}}(|g_+\rangle_{N+1}|W_+\rangle_N + |g_-\rangle_{N+1}|W_-\rangle_N)|0\rangle, \tag{18}$$

where T_2 is the time required to complete this adiabatic evolution, and we will give its calculation in the following sections. Then, we probe the state of the mural pixel $N + 1$. If it is detected to be in state $|g_+\rangle_{N+1}$, then the state of the remaining N mural pixels is reduced to the following state:

$$|W_+\rangle_N = \frac{1}{\sqrt{N}}(|e_+\rangle_1|g\rangle_2 \cdots |g\rangle_N + |g\rangle_1|e_+\rangle_2 \cdots |g\rangle_N + \cdots + |g\rangle_1|g\rangle_2 \cdots |e_+\rangle_N). \tag{19}$$

If the $N + 1$-th mural pixel is detected to be in state $|g_-\rangle_{N+1}$, the states of the remaining NV-shaped mural pixels collapse to the following state:

$$|W_-\rangle_N = \frac{1}{\sqrt{N}}(|e_-\rangle_1|g\rangle_2 \cdots |g\rangle_N + |g\rangle_1|e_-\rangle_2 \cdots |g\rangle_N + \cdots + |g\rangle_1|g\rangle_2 \cdots |e_-\rangle_N). \tag{20}$$

(a) Original image

(b) Image with noise removed

(c) Image after restoration

Figure 8: Color restoration example image.

It can be seen from this that we can obtain the W state of N mural pixels through the above operation. The probability of obtaining the state $|W_+\rangle_N$ or $|W_-\rangle_N$ is 1/2; that is, no matter the detection result of the $N+1$-th mural pixel point we get is $|g_+\rangle_{N+1}$ or $|g_-\rangle_{N+1}$, we can obtain an N mural pixel point W state. It is just that the specific form of the obtained W state depends on the detection result of the $(N+1)$-th mural pixel. The choices of $\Omega_1(t)$ and $\Omega_2(t)$ are similar to those in the previous maximum entangled states of the two mural pixels.

$$\Omega_1(t) = g_{10}\exp\left(-(vt)^2/W_c^2\right),$$
$$\Omega_2(t) = g_{20}\exp\left(-v^2(t+\tau)^2/W_c^2\right)\cos\left(\frac{2\pi z_0}{\lambda}\right). \tag{21}$$

Figure 4(a) shows the variation curve of the coupling constant of the cavity mode with time, where the pulse parameters are the same as those in Figure 3(a).

Figure 4(b) shows the variation curve of population with time when $N=4$. It can be clearly seen from the figure that all the populations are completely transferred from the initial state to $|D_2(T_2)\rangle = 1/\sqrt{2}(|g_+\rangle_{N+1}|W_+\rangle_N + |g_-\rangle_{N+1}|W_-\rangle_N)|0\rangle$. After state detection for atom $N+1$, we will get the W state of N fresco pixels.

Finally, we analyze the experimental feasibility of this scheme. The cavity field is always in the vacuum state no matter in the two-wall mural pixel entanglement state or in the N-atom W state generation scheme. Therefore, the effect of decoherence caused by the attenuation of the cavity field can be ignored. We only need to consider the effect of spontaneous emission of mural pixels. Optical cavities in the wavelength range of 630-850 nm have been experimentally realized, and the coupling constant of mural pixel cavity in this optical cavity can reach the maximum $2\pi \times 750$ MHz. The interaction time between the mural pixels and the cavity field is about $t = T_1 = T_2 \approx W_c/v = 15ns$. It can be seen from this that the generation time of the W state of the N atom has nothing to do with the number of mural pixels N we

Table 1: Effect evaluation of the color research system of Qiuci murals based on intelligent digital image processing technology.

Num	System assessment
1	70.99
2	72.67
3	67.31
4	67.46
5	68.18
6	67.86
7	76.55
8	72.72
9	76.04
10	66.00
11	76.26
12	80.79
13	73.44
14	76.71
15	69.00
16	69.95
17	68.16
18	71.69
19	79.41
20	68.92
21	74.04
22	67.49
23	65.74
24	68.10
25	69.46
26	77.59
27	67.92
28	74.66
29	72.90
30	76.12
31	65.90
32	68.50
33	78.17
34	71.67
35	80.59
36	75.22
37	71.22
38	77.24
39	65.41
40	79.09
41	79.43
42	78.35
43	76.18
44	74.95
45	74.34
46	71.26
47	64.23
48	68.81
49	66.22
50	66.58
51	75.22
52	64.43
53	71.10
54	69.81
55	75.79
56	78.16
57	74.86
58	75.86
59	69.42
60	78.43
61	77.70
62	66.32
63	78.27
64	75.70
65	68.61
66	66.04

choose; that is, the time to complete the scheme will not increase when we increase the number of mural pixels N, which can be used to achieve scalable N fresco pixel W states.

We choose cesium atom ^{133}Cs, whether it is a Λ-shaped mural pixel or a V-shaped mural pixel; it can be obtained by selecting the initial state of the mural pixel, as shown in Figure 5. We assume that the cavity-soil coupling levels are $6^2S_{1/2}$, $F = 4$ and $6^2P_{3/2}$, $F = 5$. If the mural pixel is initially prepared at the fine energy level $6^2P_{3/2}$, $F = 5, m = 0$, the effect of the mural pixel and the cavity mode is the interaction of a Λ-type mural pixel and the cavity mode, as shown in Figure 5(a). If the mural pixel is initially prepared in state $6^2S_{1/2}$, $F = 4$, $m = 0$, the effect of the mural pixel and the cavity field is a V-shaped interaction between the mural pixel and the cavity mode, as shown in Figure 5(b).

The typical fresco pixel radiation time of the excited state of our chosen fresco pixel is $t_r = 30$ ns. Therefore, the time required for our entangled state generation scheme is less than the decay time of spontaneous emission of mural pixels. In the interaction process, the cavity field is tuned to the resonance wavelength of the mural pixel at 852.36 nm, so the cavity decrement time is $t_c = 0.6 \times 10^{-6}s \gg t$. Comparing these two characteristic times, we can get the time range for completing our entangled state generation scheme: $t < t_r$. When the adiabatic condition is satisfied, the interaction time can be within an allowable range without precise control. Therefore, our scheme is experimentally feasible.

In addition, we analyze the completion efficiency of our entangled state generation scheme. We mainly take the generation process of the entangled state of two mural pixels as an example to illustrate. No matter in the two-mural pixel

point entanglement scheme or in the N mural pixel point W state generation scheme, a photon initially radiated from the Λ mural pixel point in the excited state plays a crucial role in the formation of the entanglement. It has been pointed out in the literature that an unpolarized photon source can be replaced by the radiation of two fresco pixels prepared by a laser pulse in their corresponding excited states. Moreover, the radiation process of cesium mural pixels trapped in optical cavities has been used as a single-photon source to generate the polarized photons we need. Since the spontaneous emission of mural pixels is random and cannot be directly controlled, we can use a method similar to that in the literature to improve our chances of obtaining radiated photons in the cavity by repeating the radiation process.

The specific method is as follows: the first mural pixel is irradiated with a beam of π-polarized laser pulse, and the laser is coupled to the initial state $6^2S_{1/2}, F = 4, m = 0$ of the mural pixel, and the mural pixel is set to its excited state $6^2P_{3/2}, F = 5, m = 0$. The mural pixels in the excited state will emit photons, and we assume that only the photons along the axis are collected, and the π-polarized radiation photons are not collected. In this way, only photons decaying to the point state $6^2S_{1/2}, F = 4, m = \pm 1$ of the mural pixel are observed. Since these spontaneous emission processes are the same in all other degrees of freedom except the polarization direction, we can assume that the coupling constants of the cavity mold soil and the transition of the same mural pixel point are equal. Since the observed probability of a photon with a certain polarization is less than 1, the entire radiation process needs to be repeated to increase the probability of obtaining a photon with a certain polarization.

Once a photon of a certain polarization is observed, our entire entangled state generation process may be completed.

4. Research and Application of Color of Qiuci Murals Based on Intelligent Digital Image Processing Technology

After the algorithm processing in the third part, the larger cracks in the murals of Qiuci can be accurately extracted. However, some finer cracks are not effective in the early detection, and the cracks cannot be completely extracted. In this way, the unextracted crack area will affect the effect of the subsequent rock art restoration, resulting in a certain restoration error. Therefore, in this paper, the expansion operation is performed for particularly small cracks, and the extraction area of the crack is correspondingly increased, which reduces the bad influence on the subsequent repair due to incomplete crack extraction. After the above introduction, the implementation process of this algorithm is shown in Figure 6.

The color restoration process of Qiuci murals based on intelligent digital image processing technology proposed in this paper is shown in Figure 7.

On the basis of the above research, the effect of the color restoration method of Qiuci murals based on intelligent digital image processing technology proposed in this paper is verified. In this paper, two groups of experiments are used to verify the color restoration method of Qiuci murals based on intelligent digital image processing technology. First, the color restoration effect of the method proposed in this paper is verified, as shown in Figure 8.

On the basis of the above research, the effect evaluation of the Qiuci mural color research system based on intelligent digital image processing technology is carried out, and the statistical evaluation results are shown in Table 1.

From the above research, it can be seen that the color research system of Qiuci murals based on intelligent digital image processing technology proposed in this paper has good effects and can play an important role in the digital protection and digital restoration of art.

5. Conclusion

The purpose of image restoration is to restore the original image, use the damaged image as information, repair and supplement the damaged image according to a certain rule, and remove the redundant objects in the image. The virtual repair method is used for the image to be repaired to achieve the purpose of restoration or modification, which can be used for the removal of characters, characters or obstacles, the filling or completion of image information, and the masking of some part of the image information. After years of in-depth research by researchers, the development of this technology has gradually matured. This paper combines digital technology to apply intelligent digital image processing technology to the color research of Qiuci murals and builds an intelligent system. The research results show that the color research system of Qiuci murals based on intelligent digital image processing technology proposed in this paper has good effects and can play an important role in digital art protection and digital restoration.

Data Availability

The labeled dataset used to support the findings of this study are available from the corresponding author upon request.

Conflicts of Interest

The authors declare no competing interests.

Acknowledgments

This study is sponsored by the Autonomous Region Social Science Fund, Research on the Innovation Path of Aesthetic Education in Xinjiang Colleges and Universities from the Perspective of "Culture Enriching Xinjiang," Project No. 20BYS143.

References

[1] Q. Wan, S. S. Song, X. H. Li et al., "The visual perception of the cardboard product using eye-tracking technology," *Wood Research*, vol. 63, no. 1, pp. 165–178, 2018.

[2] N. McCartney and J. Tynan, "Fashioning contemporary art: a new interdisciplinary aesthetics in art-design collaborations,"

Journal of Visual Art Practice, vol. 20, no. 1-2, pp. 143–162, 2021.

[3] J. Lockheart, "The importance of writing as a material practice for art and design students: a contemporary rereading of the coldstream reports," *Art, Design & Communication in Higher Education*, vol. 17, no. 2, pp. 151–175, 2018.

[4] G. Sachdev, "Engaging with plants in an urban environment through street art and design," *Plants, People, Planet*, vol. 1, no. 3, pp. 271–289, 2019.

[5] Y. M. Andreeva, V. C. Luong, D. S. Lutoshina et al., "Laser coloration of metals in visual art and design," *Optical Materials Express*, vol. 9, no. 3, pp. 1310–1319, 2019.

[6] Z. Nebessayeva, K. Bekbolatova, K. Mussakulov, S. Zhanbirshiyev, and L. Tulepov, "Promotion of entrepreneurship development by art and design by pedagogy," *Opción*, vol. 34, no. 85-2, pp. 729–751, 2018.

[7] D. Mourtzis, "Simulation in the design and operation of manufacturing systems: state of the art and new trends," *International Journal of Production Research*, vol. 58, no. 7, pp. 1927–1949, 2020.

[8] K. W. Klockars, N. E. Yau, B. L. Tardy et al., "Asymmetrical coffee rings from cellulose nanocrystals and prospects in art and design," *Cellulose*, vol. 26, no. 1, pp. 491–506, 2019.

[9] M. Hermus, A. van Buuren, and V. Bekkers, "Applying design in public administration: a literature review to explore the state of the art," *Policy & Politics*, vol. 48, no. 1, pp. 21–48, 2020.

[10] J. Calvert and P. Schyfter, "What can science and technology studies learn from art and design? Reflections on 'synthetic aesthetics'," *Social Studies of Science*, vol. 47, no. 2, pp. 195–215, 2017.

[11] J. A. Greene, R. Freed, and R. K. Sawyer, "Fostering creative performance in art and design education via self-regulated learning," *Instructional Science*, vol. 47, no. 2, pp. 127–149, 2019.

[12] B. Bafandeh Mayvan, A. Rasoolzadegan, and Z. Ghavidel Yazdi, "The state of the art on design patterns: a systematic mapping of the literature," *Journal of Systems and Software*, vol. 125, no. C, pp. 93–118, 2017.

[13] A. Thorpe and E. Manzini, "Weaving people and places: art and design for resilient communities," *She Ji: The Journal of Design, Economics, and Innovation*, vol. 4, no. 1, pp. 1–10, 2018.

[14] M. Sclater and V. Lally, "Interdisciplinarity and technology-enhanced learning: reflections from art and design and educational perspectives," *Research in Comparative and International Education*, vol. 13, no. 1, pp. 46–69, 2018.

[15] V. Kinsella, "The use of activity theory as a methodology for developing creativity within the art and design classroom," *International Journal of Art & Design Education*, vol. 37, no. 3, pp. 493–506, 2018.

[16] C. Liu, S. Chen, C. Sheng, P. Ding, Z. Qian, and L. Ren, "The art of a hydraulic joint in a spider's leg: modelling, computational fluid dynamics (CFD) simulation, and bio-inspired design," *Journal of Comparative Physiology A*, vol. 205, no. 4, pp. 491–504, 2019.

[17] Z. Luo and J. Dai, "Synthetic genomics: the art of design and synthesis," *Synthetic genomics: the art of design and synthesis. Sheng wu gong cheng xue bao= Chinese journal of biotechnology*, vol. 33, no. 3, pp. 331–342, 2017.

[18] E. Knight, J. Daymond, and S. Paroutis, "Design-led strategy: how to bring design thinking into the art of strategic management," *California Management Review*, vol. 62, no. 2, pp. 30–52, 2020.

[19] D. Jordan and H. O'Donoghue, "Histories of change in art and design education in Ireland: towards reform: the evolving trajectory of art education," *International Journal of Art & Design Education*, vol. 37, no. 4, pp. 574–586, 2018.

[20] J. H. Zou and X. M. Hu, "Entangled atomic state generation via adiabatic evolution of dark eigenstates in cavity QED," *Optics Communications*, vol. 281, no. 19, pp. 5067–5071, 2008.